

# Post-transplant upregulation of chemokine messenger RNA in non-human primate recipients of intraportal pig islet xenografts

Hårdstedt M, Finnegan CP, Kirchhof N, Hyland KA, Wijkstrom M, Murtaugh MP, Hering BJ. Post-transplant upregulation of chemokine messenger RNA in non-human primate recipients of intraportal pig islet xenografts.

Xenotransplantation 2005; 12: 293–302. © Blackwell Munksgaard, 2005

**Abstract:** Background: We have previously shown that pig-to-primate intraportal islet xenografts reverse diabetes, escape hyperacute rejection, and undergo acute cellular rejection in non-immunosuppressed recipients. To gain a better understanding of mechanisms contributing to xenograft rejection in non-human primates we examined gene expression in livers bearing islet xenografts in the first 72 h after transplantation.

**Methods:** Liver specimens were collected at sacrifice from seven non-immunosuppressed rhesus macaques at 12, 24, 48 and 72 h after intraportal porcine islet transplantation. Following total RNA extraction, mRNA was quantified using SYBR green real-time reverse transcription polymerase chain reaction (RT-PCR) for species-specific immune response genes. Data were analyzed using comparative cycle threshold (Ct) analysis, adjusted for specific primer-efficiencies and normalized to cyclophilin expression.

**Results:** Porcine insulin mRNA was detected in all liver samples. Cluster analysis revealed differential gene expression patterns at 12 and 24 h (early) compared with at 48 and 72 h (late) post-transplant. Gene expression patterns were associated with histological findings of predominantly neutrophils and only a few lymphocytes at 12 and 24 h and an increasing number of lymphocytes and macrophages at 48 and 72 h. Transcript levels of CXCR3 and its ligands, interferon-inducible protein 10 (IP-10) and monokine induced by IFN- $\gamma$  (Mig), significantly increased between early and late time points together with expression of MIP-1 $\alpha$ , regulated on activation normal T expressed and secreted protein (RANTES) and MCP-1. CCR5 showed only a marginal, non-significant increase. Fas ligand, perforin and granzyme B transcripts were all elevated at 48 and 72 h post-transplant.

**Conclusions:** Our data suggest that CXCR3, with ligands IP-10 and Mig, is involved in T cell recruitment in acute islet xenograft rejection in non-human primates. Upregulation of RANTES and MIP-1 $\alpha$  transcripts in the absence of a significant CCR5 increase suggests a possible involvement of other chemokine receptors. MCP-1 expression is associated with T cell and macrophage infiltration. Elevated cytotoxic effector molecule expression (Fas ligand, perforin, granzyme B) indicates T-cell mediated graft destruction by cytotoxic and cytolytic mechanisms within 48 to 72 h after transplantation. These results identify the CXCR3-mediated chemoattractant pathway as an immunosuppressive target in pig-to-primate islet xenotransplantation.

**Maria Hårdstedt,<sup>1,2</sup> Colleen P. Finnegan,<sup>3</sup> Nicole Kirchhof,<sup>1</sup> Kendra A. Hyland,<sup>3</sup> Martin Wijkstrom,<sup>1</sup> Michael P. Murtaugh<sup>3</sup> and Bernhard J. Hering<sup>1</sup>**

<sup>1</sup>Diabetes Institute for Immunology and Transplantation, Department of Surgery, University of Minnesota, Minneapolis MN, <sup>2</sup>Department of Clinical Immunology, Rudbeck Laboratory, Uppsala University Hospital, Uppsala, Sweden, <sup>3</sup>Department of Veterinary and Biomedical Sciences, University of Minnesota, St Paul, MN, USA

**Key words:** chemokines – CXCR3 – intragraft gene expression – islet xenograft rejection – non-human primate – xenotransplantation

**Abbreviations:** Ct: cycle threshold; FasL: Fas ligand; GB: granzyme B; I-TAC: T-cell  $\alpha$  chemoattractant, CXCL11; IP-10: interferon-inducible protein 10, CXCL10; Mig: monokine induced by IFN- $\gamma$ , CXCL9; MIP-1 $\alpha$ : macrophage inflammatory protein, CCL3; MIP-1 $\beta$ : macrophage inflammatory protein, CCL4; NHP: non-human primate; PBMCs: peripheral blood mononuclear cells; PCR: polymerase chain reaction; RANTES: regulated on activation normal T expressed and secreted protein, CCL5; rhesus monkey: *Macaca mulatta*; RT-PCR: reverse transcription polymerase chain reaction; TNF- $\alpha$ : tumor necrosis factor alpha.

Address reprint requests to Maria Hårdstedt, Department of Clinical Immunology, Rudbeck Laboratory, Uppsala University Hospital, SE-75185 Uppsala, Sweden (E-mail: maria.hardstedt@klinimm.uu.se)

Received 19 January 2005;  
Accepted 10 March 2005

## Introduction

Recent advances in human islet transplantation have documented the potential of cell-based diabetes therapy but have also emphasized the need for a more widely available source of donor tissue. Xenogeneic porcine islets provide such a source but their utilization will require a better understanding of the immunobiology of islet xenotransplantation as a basis for the rational design of immunosuppressive regimens. Rejection mechanisms in murine recipients of islet xenografts are becoming increasingly defined [1,2] but mechanisms leading to rejection of intraportal porcine islet xenotransplants in non-human primates (NHPs) remain poorly understood [3–5]. Among the immune mediators that are present at the graft site, chemokines have gained special interest due to their ability to recruit and activate immune cells and initiate the immune response resulting in rejection [6,7]. Species differences in chemokine/chemokine receptor function and expression underline the importance of studying these events in a model closer to the clinical setting [8].

We have previously shown that intraportal porcine islet xenografts temporarily reverse diabetes in non-immunosuppressed rhesus monkeys [5]. Our histopathological and immunohistological findings suggested that islet xenografts are subjected to early deposition of immunoglobulins and complement as well as an early infiltration of neutrophils [5]. The majority of transplanted islets did undergo cellular rejection mediated by CD4<sup>+</sup> and CD8<sup>+</sup> T cells and macrophages starting at 24 to 48 h post-transplant with severe ongoing rejection of the xenograft by 72 h [5].

To delineate critical events in leukocyte recruitment and graft destruction, we examined intra-graft mRNA expression of selected myeloid and lymphoid cell-attracting chemokines, chemokine receptors, inflammatory cytokines, T cell markers and cytotoxic effector molecules. Our results indicate a major involvement of CXCR3-mediated chemotaxis [CXCR3, interferon-inducible protein 10 (IP-10), monokine induced by IFN- $\gamma$  (Mig)] and suggest an important role for the chemokines regulated on activation normal T expressed and secreted protein (RANTES), MIP-1 $\alpha$  and MCP-1 in recruitment of T cells and macrophages to the xenograft. Elevation of cytotoxic effector molecule mRNA expression implies that T cell mediated cytotoxic and cytolytic mechanisms are active within 48 to 72 h post-transplant.

## Methods

### Animal model

Seven female rhesus macaques were used as recipients and seven adult Landrace sows (> 2 yr) were used as pig donors [5]. Diabetes was induced in five of the seven NHPs (excluding recipient 98EP6 and 98EP7) by intravenous administration of streptozotocin (STZ). Plasma glucose concentrations were measured twice daily and controlled by administration of intravenous insulin pre-transplant. No insulin was given post-transplant and none of the seven recipients received immunosuppressive therapy prior to or after islet transplantation. Porcine islets were isolated as described [5]. After 48 h culture, 20 000 islet equivalents (IE)/kg were infused into a mesenteric tributary to the portal vein following mini-laparotomy [5]. Islet graft functional status was determined by glycemic control and porcine C-peptide measurements. Transplanted porcine xenografts promptly reversed diabetes in diabetic recipients, glycemic control was maintained throughout the short follow-up period and all recipients were normoglycemic at the time of sacrifice [5]. Animals were killed at 12 (n = 2; 98EP1 and 98EP6), 24 (n = 2; 68Q and 98EP7), 48 (n = 2; 98EP9 and 98EP10), and 72 h (n = 1; 98EP5) post-transplant. A thromboembolic event occurred in recipient 98EP1; thrombus in the jugular vein extending from an indwelling catheter resulted in multiple thrombi in the lung and a disseminated inflammatory reaction. This recipient was excluded from further analysis.

### RNA isolation and reverse transcription

Liver tissue was collected from random locations at sacrifice, snap frozen and stored at -80 °C. RNA was extracted from 600 mg pieces of liver tissue using the RNeasy kit (Qiagen, Valencia, CA, USA). Total RNA was quantified using a spectrophotometer and validated by RNA 6000 Nano LabChip technology (Agilent Technologies, Palo Alto, CA, USA). Reverse transcription was performed using 2  $\mu$ g of total RNA according to the Invitrogen SuperScript<sup>TM</sup> II RNase H<sup>-</sup> reverse transcriptase protocol (Invitrogen, Carlsbad, CA, USA).

### Species-specific real-time polymerase chain reaction (PCR)

Species-specific intron-spanning primers for monkey and pig sequences were designed using Primer 3 software (Whitehead Institute, Cambridge, MA,

Table 1. Oligonucleotide primers used in real-time reverse transcription polymerase chain reaction

Gene	Genbank accession number	Forward sequence	Reverse sequence	Product size (bp)	Product melting temperature (T <sub>m</sub> , °C)
<b>Non-human primate primers</b>					
Cyclophilin	AF023861	5' aattattccagggttatgtgt 3'	5' ctgggaaccattgtgtgggt 3'	167	80.1 to 80.3
CXCR3	NM_001504	5' caaccacaagcaccacaagc 3'	5' aacctcgccgtcatttagc 3'	115	84.3 to 84.5
CCR5	NM_000579	5' catccgttcccctacaagaa 3'	5' ggcagggtcccgatgataa 3'	102	77.3 to 78.0
CCR7	NM_001838	5' cccagagagcgtcatgg 3'	5' tccactgtgtgtgtctcc 3'	132	82.1 to 82.5
CD8-α	NM_001768	5' gggctcttctctgctcaactg 3'	5' gtctcccatttgaccacag 3'	105	80.3 to 80.9
CD4	M31134	5' agggagatcccaattgcag 3'	5' aatcgtagaggaggcgaaca 3'	125	83.5 to 84.0
MCP-1 (CCL2)	NM_002982	5' acttcaccaataggaagatctcag 3'	5' gcttgccagggtggtccatggaatcctga 3'	170	82.5 to 82.6
MIP-1α (CCL3)	NM_002983	5' gagacgagcagccactgac 3'	5' gacatatttctggaccactcc 3'	102	82.5 to 83.0
Mip-1β (CCL4)	NM_002984	5' ctgtctgtctctctcatgc 3'	5' cacaagttgcccaggaagc 3'	128	81.9 to 82.5
RANTES (CCL5)	NM_002985	5' agtggcaagtgtccaacc 3'	5' cgaaccatttctctctgg 3'	86	80.2 to 80.8
IL-8 (CXCL8)	NM_000584	5' gaactgagagtgattgagatgg 3'	5' aaacttcccacaacctctgc 3'	126	80.4 to 80.7
Mig (CXCL9)	NM_002416	5' aagggactatccacctacaatcc 3'	5' cttcacatctgctgaatctgg 3'	137	76.5 to 76.7
IP-10 (CXCL10)	NM_001565	5' tcaagaatttactgaaagcagttagc 3'	5' ctgtgtgtccatccttg 3'	104	76.1 to 76.7
I-TAC (CXCL11)	NM_005409	5' gatgcctaaatcccaaatcg 3'	5' cagtagtcacagttaaactgttctagg 3'	140	74.4 to 75.0
TNF-α	U19850	5' ttctgtctgtgcaacttgg 3'	5' tcgagaagatgatctgactg 3'	105	82.2 to 82.5
IL-1β	U19845	5' ggacaatgacctgagcacct 3'	5' accaagctttgagctgtgc 3'	133	81.6 to 81.8
Granzyme B	XM_032600	5' ggcttctgatacagagacga 3'	5' gtcggctctctgtcttctgat 3'	128	81.7 to 82.1
Fas-L	AB035139	5' gggatgttccagctctcca 3'	5' tggggtagcatttcttc 3'	106	80.0 to 80.4
Perforin	M28393	5' aagaccaccaggaccagta 3'	5' ctcttgaagtcagggtgcag 3'	104	82.6 to 82.9
<b>Pig primers</b>					
Cyclophilin	AY008846	5' ccgctgatggcagcccc 3'	5' cccgtatgcttcaggataaaa 3'	250	82.2 to 82.3
IL-1β	M86725	5' cctctcccaggcctcttgt 3'	5' gggccagccagcactagaga 3'	175	80.8 to 81.1
Insulin	AF064555	5' gcttctctacagcccaag 3'	5' cacttgcctgagggttctc 3'	54	81.3 to 81.9

USA) (Table 1). Primers were validated and cross-specificity was confirmed using genomic DNA and cDNA from activated peripheral blood mononuclear cells (PBMCs) isolated from human, rhesus monkey and pig (Fig. 1). Amplification of the desired PCR product was verified by agarose gel

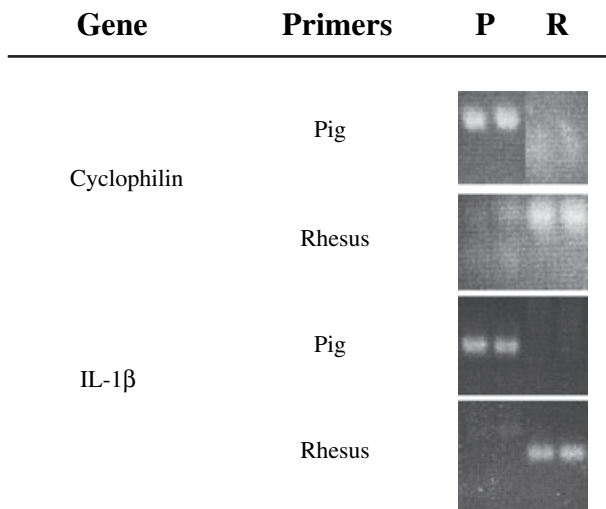


Fig. 1. Validation of real-time reverse transcription polymerase chain reaction assays. Species-specific amplification of porcine (P) and rhesus monkey (R) cyclophilin and IL-1β. Reactions containing 6 to 10 ng of activated PBMC cDNA were run for 50 cycles. Six microliter of the reaction product were electrophoresed on an agarose gel and stained with ethidium bromide. Results were confirmed by specific melting temperature analysis.

electrophoresis and specific melting temperature given by Dissociation Curve 1.0 software (Applied Biosystems, Foster City, CA, USA). Real-time PCR was performed in 15 μl containing 6 to 10 ng cDNA, 50 to 100 nM primers and 2xSYBR Green Master Mix (Applied Biosystems) and run on an ABI Prism 7700 or 7790 Sequence Detection System (Applied Biosystems). Thermocycler conditions were 95 °C for 10 min followed by 50 cycles of 95 °C for 15 s and 60 °C for 1 min. Data were analyzed by the comparative threshold cycle (Ct) method [9] with adjustments for average amplification efficiencies as determined with LinReg software (outliers excluded using the KOD method) [10, 11]. Data are presented as the expression ratio of target gene to cyclophilin ( $\text{Eff}_{\text{target}}^{-\text{Ct}(\text{target})} / \text{Eff}_{\text{cyclophilin}}^{-\text{Ct}(\text{cyclophilin})}$ ) and relative fold change differences between samples after normalizing to expression of cyclophilin.

Histopathology and immunohistochemistry

Morphological studies were performed for formalin-fixed and frozen liver tissue samples as previously described [5]. Intrahepatic islet xenografts were divided into four categories depending on intactness and leukocyte infiltration as follows: (A) well-preserved islet without infiltrate; (B) islet present, but islet damage or islet-associated leukocytes corresponding to < 50% of islet area;

(C) insulin-positive cells present, but damage or infiltrate corresponding to > 50% of islet area and (D) infiltrate only, without insulin-positive cells. An avidin-biotin-peroxidase detection system (Dako, Carpinteria, CA, USA) was used for immunohistochemical labeling of various cell types in the infiltrate [5].

Data analysis

Due to the exponential characteristics of real-time PCR data, statistical analysis was performed after log<sub>2</sub> transformation. Hierarchic cluster analysis of gene expression data was performed using Cluster and TreeView software (Eisen, Stanford University) [12]. Transcript levels were correlated to histological estimation of cell infiltration at the graft site (% category D islets, as defined above) using Pearson correlations. Statistical significance levels were \*P < 0.05 and \*\*P < 0.01.

Results

Porcine-specific gene expression

As previously reported, histopathology revealed numerous xenogeneic islets in the liver at sacrifice for all recipients [5]. By designing species-specific real-time reverse transcription polymerase chain reaction (RT-PCR) assays we were able to define donor and recipient derived gene expression

(Fig. 1). Pig-specific cyclophilin mRNA and porcine insulin mRNA were detected in all liver tissue samples confirming the presence of intra-hepatic porcine tissue and porcine islet cells, respectively. The ratio of species-specific pig to rhesus cyclophilin mRNA was between 1 : 500 and 1 : 900.

Differential immune gene expression at 12 and 24 h vs. 48 and 72 h post-transplant

Cluster analysis of all immune response genes in the study revealed two distinct expression patterns when comparing recipients killed at 12 and 24 h with recipients killed at 48 and 72 h post-transplant (Fig. 2). Immunopathological findings showed a significant increase of CD4+ and CD8+ T cells and macrophages between the two early and late time points (Fig. 3) [5]. Very few T cells were present at 12 h and the number slightly increased at 24 h. Macrophages were observed rarely at 12 h and at 24 h [5]. At 48 and 72 h the dominant cells infiltrating and colocalizing with the islet grafts were T cells with an almost equal number of macrophages at 72 h (Fig. 3) [5]. To delineate immune mechanisms contributing to and activated during cell infiltration, mRNA transcript levels for selected immune response genes were compared between animals killed at 12 to 24 h (early) and at 48 to 72 h (late) (Table 2). Transcript levels of the immune

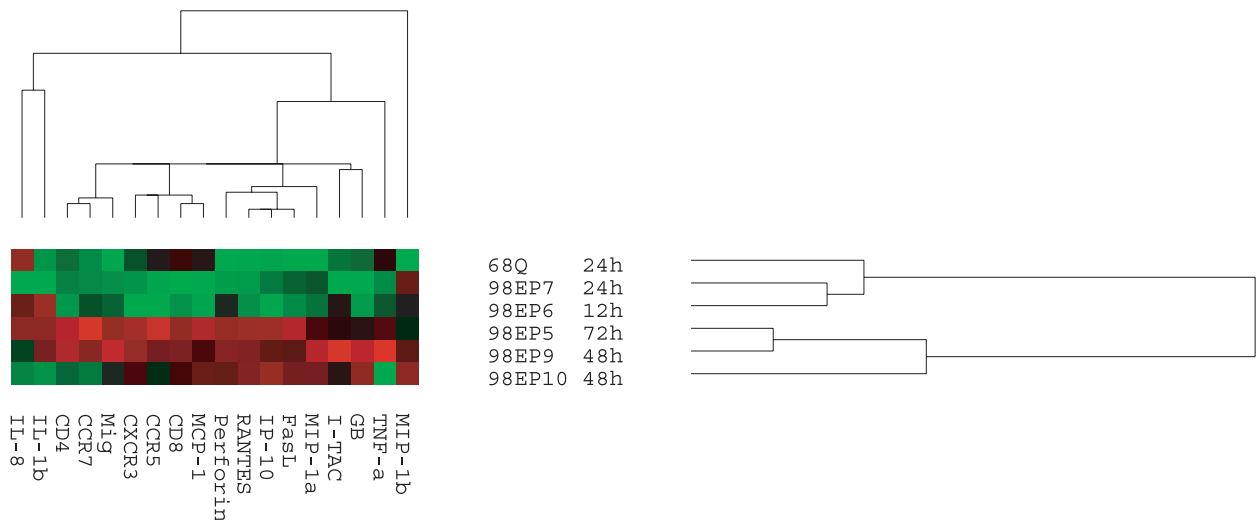


Fig. 2. Cluster analysis based on gene expression results (ratio of target to cyclophilin mRNA expression) for 18 monkey immune response genes. Agglomerative, hierarchical cluster analysis was performed using the average-linkage method after log<sub>2</sub>-transformation, normalization and mean centering of genes using Cluster (Eisen, Stanford University). Results were displayed with TreeView (Eisen, Stanford University). Elevated expression levels, compared with average, are shown in increasing intensities of red and reduced levels are shown in green. No change is black. The dendrogram divides the recipients in two distinct groups according to early and late sacrifice. Undetected values for GB were assigned an arbitrary endpoint level of detection (Ct = 50) for statistic analysis.

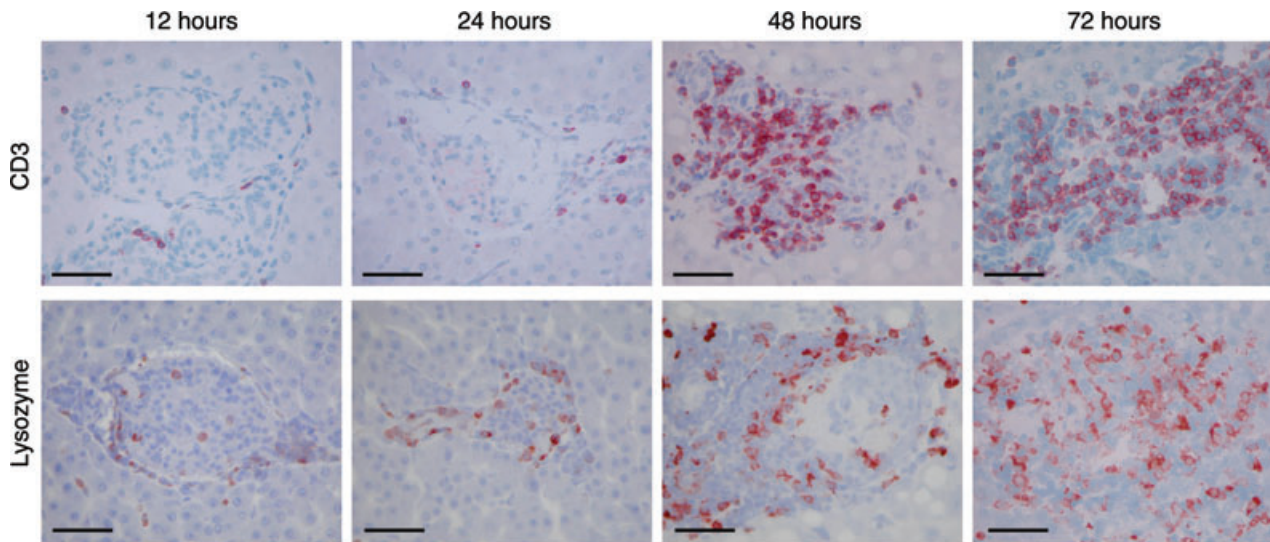


Fig. 3. Immunostaining for infiltrating T cells and macrophages of liver specimens obtained at 12, 24, 48, and 72 h after intraportal porcine islet xenotransplantation in non-immunosuppressed non-human primates. Islets from 12 and 24 h display few CD3<sup>+</sup> T cells, and some lysozyme<sup>+</sup> cells, either macrophages or polymorphonuclear granulocytes. At 48 and 72 h, significantly more T cells and macrophages are present. Neutrophil elastase staining at 48 and 72 h was practically negative (not shown). Bars = 50  $\mu$ m.

Table 2. Gene expression analysis after NHP islet xenotransplantation

Gene	Target/cyclophilin (mRNA expression $\times 10^6$ in late group) <sup>a</sup>	Fold change increase (late/early) <sup>b</sup>	Correlation ( <i>r</i> ) with %D islets <sup>c</sup>
CXCR3	44	13.7*	0.88*
IP-10	1377	29.8**	0.84*
Mig	2106	9.4*	0.98**
I-TAC	21	4.6	n.s.
CCR5	32	1.9	n.s.
MIP-1 $\alpha$	27	19.4*	0.85*
MIP-1 $\beta$	4.1	6.5	n.s.
RANTES	284	4.6**	0.91*
CD4	3120	2.0	0.93**
CD8 $\alpha$	99	3.9	n.s.
FasL	6.7	3.3**	0.91*
Perforin	108	3.7*	0.91*
GB <sup>d</sup>	$2.5 \times 10^{-5}$	14.3*	n.d.
CCR7	75	2.8	0.92**
MCP-1	674	2.7*	n.s.
IL-8	66	0.94	n.s.
TNF- $\alpha$	260	1.7	n.s.
IL-1 $\beta$	353	1.3	n.s.

<sup>a</sup>Expression levels are given as geometric means of ratios (target/cyclophilin) mRNA in recipients killed at 48 and 72 h.

<sup>b</sup>Fold change difference in transcript levels comparing animals killed at 12 to 24 h (early) and 48 to 72 h (late) post-transplant. Fold change difference is based on the geometric means and significance was determined by Student's *t*-test; \**P* < 0.05, \*\**P* < 0.01.

<sup>c</sup>Pearson correlation coefficients (*r*) between gene expression levels and percentage of islets defined as category D (see Methods); \**P* < 0.05, \*\**P* < 0.01.

<sup>d</sup>GB was not detected (n.d.) in early samples. Fold change was calculated using an arbitrary baseline level of detection based on a cycle threshold (Ct) value of 50. n.s., not significant.

response genes were correlated with percentage of category D islets classified as heavily infiltrated by leukocytes [5].

CXCR3- and CCR5-mediated chemokine pathways

The CXCR3 and its ligands IP-10 and Mig, showed an average increase in mRNA expression of 14-fold, 30-fold and 9-fold, respectively when comparing animals killed early and late (Table 2; Fig. 4A). CXCR3 showed the highest expression at 72 h (recipient 98EP5), 69-fold greater than the level at 12 h (Fig. 4D). For the same recipient IP-10 was increased 60-fold and Mig 9-fold compared with at 12 h. IP-10 and Mig reached the highest relative level of expression of all chemokines studied (Fig. 5). CXCR3 mRNA correlated with expression of IP-10 and Mig mRNA (*r* = 0.82 and 0.86, *P* < 0.05), but not with T-cell  $\alpha$  chemoattractant-CXCL11 (I-TAC). The increase in I-TAC expression was due to a 40-fold increase in recipient 98EP9 at 48 h; overall I-TAC levels were not significantly different (Table 2; Fig. 4A). A high degree of leukocytic infiltration of xenografts (%D islets) positively correlated with high levels of CXCR3, IP-10 and Mig transcripts, but not with expression of I-TAC (Table 2).

The CCR5 increased only marginally (*P* = 0.087) (Table 2). The highest relative increase in CCR5 expression, 3.5-fold compared with the recipient killed at 12 h, was detected at 72 h (recipient 98EP5) (Fig. 4D). In contrast, MIP-1 $\alpha$  and RANTES, both ligands to CCR5, showed significant elevations (Table 2; Fig. 4B). MIP-1 $\alpha$  and RANTES transcripts correlated positively with the degree of leukocytic infiltration (%D islets). Macrophage inflammatory protein-CCL4 (MIP-1 $\beta$ ), the third ligand of CCR5, was expressed

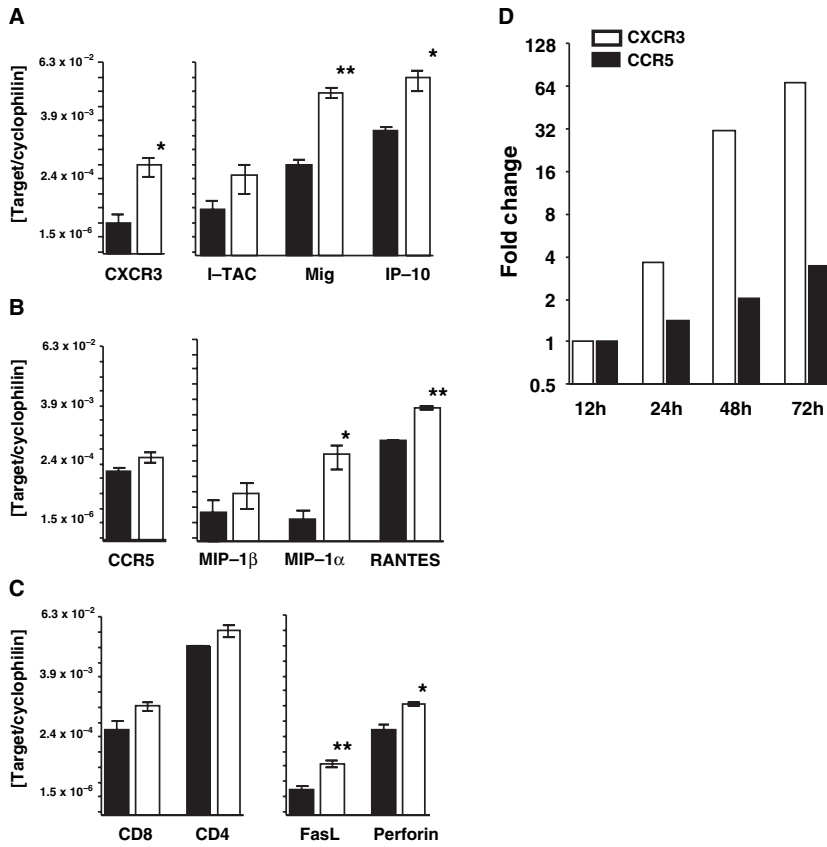


Fig. 4. Expression levels of CXCR3 and CXCR3-binding chemokine transcripts (A), CCR5 and CCR5-binding chemokine transcripts (B), and T cell markers and cytotoxic effector molecules (C) at 12 to 24 h (■) and 48 to 72 h (□) post-transplant. mRNA levels are given as mean ± SEM of the ratio of target to cyclophilin and presented on a log<sub>2</sub> scale. Significance was determined by Student's t-test; \*P < 0.05, \*\*P < 0.01. Panel D shows the relative increase in transcript levels over time for CXCR3 (□) and CCR5 (■). Data presented on a log<sub>2</sub> scale as fold-change increase in expression compared with expression level at 12 h.

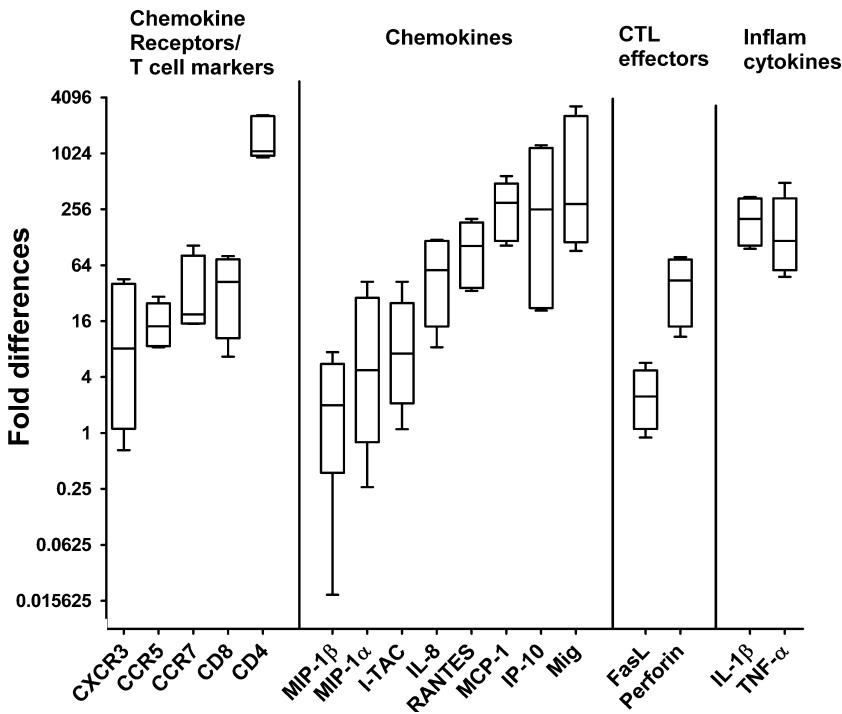


Fig. 5. Relative expression levels of immune response genes in transplanted liver tissue. Expression levels are relative to average MIP-1β expression (set to one on the y-axis) in all liver samples from 12 to 72 h post-transplant. For each gene the boxplot extends from the 25th to the 75th percentile and with a horizontal line indicating the median; whiskers show maximum and minimum values. Data are presented on a log<sub>2</sub> scale.

at low levels and showed a random variation between recipients. CCR5 and MIP-1β mRNA expression did not correlate with %D islets

(Table 2). There was also no correlation between CCR5 expression and the expression of its three ligands.

## CCR7

The CCR7 transcript levels correlated with %D islets on histology and showed a 3-fold increase between recipients killed 12 to 24 and 48 to 72 h post-transplant (Table 2).

## CD4, CD8 mRNA expression and cytotoxic effector molecule response

The increase in CD4 and CD8 expression between early and late groups tended to significance ( $P = 0.083$  and  $P = 0.073$ , respectively) within this small group of animals. CD4 mRNA showed the highest expression levels of all genes studied and it was positively correlated with %D islets (Table 2). The mRNA levels for CD4 were higher than for CD8 at all time points post-transplant (Fig. 5). However, the relative increase of CD8 transcripts was greater than for CD4 over time (Table 2). Recipients killed at 12 to 24 h post-transplant had on average a CD4/CD8 transcript ratio of 65 : 1 whereas animals killed later had a CD4/CD8 ratio of 30 : 1. Cytotoxic effector molecule transcripts, Fas ligand (FasL) and perforin, were detected at early time points and increased on average 3- to 4-fold at late time points (Table 2; Fig. 4C). Granzyme B (GB) mRNA was not detected at early times but was found at very low levels at late times (Table 2). The increase in expression of FasL and perforin strongly correlated with an increase in cell infiltration on histology (%D islets; Table 2).

## MCP-1, IL-8 and inflammatory cytokines

The MCP-1 was expressed at a high level in graft tissue (Fig. 5) and showed a significant 3-fold increase between the early and late killed recipients (Table 2). IL-8 mRNA showed variable expression between individuals and was not associated with time after transplant (Table 2; Fig. 2). Rhesus IL-1 $\beta$  mRNA levels were highest at 12 h, whereas pig IL-1 $\beta$  was undetected in all samples. The overall increase in tumor necrosis factor alpha (TNF- $\alpha$ ) mRNA was primarily due to a 6-fold increase in one recipient (98EP9 at 48 h; Table 2; Fig. 2). There was no correlation between IL-8, IL-1 $\beta$  or TNF- $\alpha$  mRNA and T cell/macrophage infiltration on histology (%D islets). As demonstrated by cluster analysis there was also no correlation between the expression of these three markers of inflammatory activity and chemokine receptor expression, chemokine expression or cytotoxic effector molecule transcript levels (Fig. 2).

## Individual variation in immune response

*Recipients killed early (12 and 24 h post-transplant)*  
Recipient 98EP6 (12 h) showed comparatively low expression levels for most genes except for IL-1 $\beta$  and IL-8, suggesting an early innate inflammatory response (Fig. 2). Recipient 98EP7 (24 h) demonstrated overall the lowest immune response mRNA levels in the group. Recipient 68Q (24 h) had higher levels of IL-8 and MCP-1 and an early influx of single CD68<sup>+</sup> macrophages based on immunohistochemistry [5]. CD8 and CXCR3 transcript levels were also higher than for the other early group recipients.

*Recipients killed late (48 and 72 h post-transplant)*  
Animals 98EP9 (48 h) and 98EP5 (72 h) showed similar expression patterns with relatively high expression levels of immune response genes (Fig. 2). Immunohistology suggested higher numbers of B cells and macrophages and lower numbers of T cells for recipient 98EP9, compared with recipient 98EP5 [5]. This cell infiltration was accompanied by relatively higher levels of I-TAC, MIP-1 $\alpha$  and TNF- $\alpha$  but lower levels of IP-10 mRNA for recipient 98EP9. Recipient 98EP10 (48 h) had low expression of CD4 mRNA whereas the levels of CD8 and cytotoxic effector molecules were similar to other recipients killed late. These findings were consistent with a lack of CD4<sup>+</sup> T cells but numerous CD8<sup>+</sup> T cells on immunohistology [5]. Recipient 98EP10 also showed a comparatively low intragraft inflammatory activity based on low expression levels of TNF- $\alpha$ , IL-1 $\beta$  and IL-8 mRNA (Fig. 2).

## Discussion

Elucidating the critical events in initiation and maturation of immune responses to islet xenografts in a pre-clinical model will facilitate the rational development of selective yet effective interventional strategies to prevent rejection. Thus, we examined intragraft gene expression events in the first 72 h after intraportal xenoislet transplantation to gain insight to the molecular basis of rejection events that were previously characterized histomorphologically [5].

The most notable finding was a significant increase of transcripts involved in the CXCR3-mediated chemotactic pathway (CXCR3, IP-10 and Mig mRNA). These results suggest a prominent involvement of CXCR3-mediated chemotaxis after xenoislet transplantation with IP-10 and Mig as main chemoattractants of CXCR3-positive cells. The absence of NK-cells in the islet infiltrates,

based on immunohistology [5], and the documented receptor-specificity of CXCR3-binding chemokines, suggest that this pathway predominantly mediates Th1/Tc1 cell chemotaxis in our model [13,14]. Several clinical and pre-clinical studies in whole organ transplantation indicate a pivotal role for CXCR3 and its ligands, predominantly IP-10 and Mig, in recruitment of T cells to the graft site [15–17]. In murine alloslet transplant models, CXCR3 and its ligands are present at sites of rejection [18–19]. Direct targeting of CXCR3-mediated chemotaxis using CXCR3<sup>-/-</sup> mice or by  $\alpha$ -IP-10 antibody treatment also moderately prolonged alloslet graft survival in mice [20]. In islet xenotransplantation few studies have explored the importance of this chemoattractant pathway. Expression of IP-10 is correlated with T cell infiltration in the pig-to-mouse model [21,22] but there appears to be no information available on CXCR3, Mig and I-TAC expression dynamics in islet xenograft rejection.

The RANTES and MIP-1 $\alpha$  mRNA were expressed at all time points and significantly increased over the 72 h study period indicating involvement in the cellular rejection process. Expression of both these chemokines correlated with a higher degree of T cell and macrophage infiltration at the graft site [5]. Intragraft expression of RANTES and MIP-1 $\alpha$  at rejection has previously been observed in the pig-to-mouse islet transplant model [21,22]. MIP-1 $\alpha$  and RANTES both interact with CCR1 and CCR5 expressed by T cells and macrophages [13,14]. RANTES also binds to CCR3 expressed by T cells [13,14]. The only marginal increase in CCR5 expression in our study indicates that this receptor is less abundant on infiltrating cells compared with CXCR3 (Fig. 3D). This may suggest a less prominent role for CCR5 in cell recruitment in intraportal islet xenotransplant rejection and that other receptors (e.g. CCR1) might be preferentially engaged in RANTES and MIP-1 $\alpha$  mediated chemotaxis at this time during the rejection process [23]. MCP-1, a chemokine specific for CCR2, was expressed at high levels in graft tissue at all time points and was significantly increased in association with cellular influx. Early expression of MCP-1 post-transplant was previously observed in murine islet allo- and xenograft models [19,21,22,24].

The importance of CCR2- and CCR5-mediated chemotaxis in islet graft rejection has recently been thoroughly examined in murine models of islet allotransplantation. Prolonged allograft survival occurs in CCR2<sup>-/-</sup> or CCR5<sup>-/-</sup> mice, or by TAK-779 (a CCR5-antagonist) treatment, but

without a synergistic enhancement when targeting both pathways [19,24,25]. Interestingly CCR5<sup>-/-</sup> deletion led to a switch from Th1 to a Th2 response in one case without a significant difference in the number of infiltration CD3<sup>+</sup> cells [25]. Targeting the MCP-1/CCR2 pathway by anti-MCP-1 monoclonal antibody treatment or by using CCR2<sup>-/-</sup> mice, in combination with low dose rapamycin, resulted in markedly prolonged islet allograft survival [19,26]. In a pig-to-mouse islet xenograft model no significant difference in cell infiltration (CD4<sup>+</sup> T cells and macrophages) was demonstrated between CCR5<sup>-/-</sup> and wild type mice whereas the CCR2<sup>-/-</sup> mice showed a delayed cell influx [22]. Whether this infiltration was a predominant Th2- or Th1-type response was not examined. These findings further indicate that CCR5 may have a less important role in islet xenotransplantation. Changes in CCR2 could not be determined as NHP-specific primer pairs amplifying both splice variants of CCR2 mRNA did not yield specific amplification products in any samples or in control tissues. However, expression of the CCR2-specific chemokine MCP-1, together with a substantial infiltration of macrophages and T cells, known to express CCR2, support the importance of MCP-1-mediated chemotaxis as proposed in murine islet allo- and xenograft models.

The CCR7 showed a significant increase in expression over the study period and a significant correlation with cell infiltration. This could be due to increased numbers of CCR7<sup>+</sup> T cells at the graft site but also may reflect receptor switch by graft infiltrating dendritic cells during maturation, enabling their migration to secondary lymphoid organs [27]. Immature dendritic cells are attracted by inflammatory chemokines, including MCP-1, MIP-1 $\alpha$  and RANTES, that are expressed early after transplantation. CCR7<sup>+</sup> T cell subsets, in addition to naive T cells, are the central-memory cells (CD45RA<sup>-</sup>CCR7<sup>+</sup>) [28]. Recent data in mice show that these cells are capable of performing cytolytic effector functions [29].

We observed increased levels of CD4 and CD8 transcripts with a concurrent increase in expression of three cytotoxic effector molecules; FasL, perforin and GB. These findings were consistent with immunohistological results showing CD4<sup>+</sup> and CD8<sup>+</sup> T cell influx to the graft from as early as 24 h post-transplant [5]. Thus, our data support an early involvement of the Fas/FasL- and perforin/granzyme-pathways after intraportal islet xenotransplantation. The involvement of CD8<sup>+</sup> T cells in islet xenotransplantation has previously been demonstrated in pig-to-mouse [30] and pig-to-NHP

models [5,31]. Also human CD4<sup>+</sup> T cells have been shown to lyse pig cells in vitro by FasL/Fas cytotoxicity [32].

In conclusion, our study is the first to analyze intragraft mRNA expression of immune response genes in livers of non-immunosuppressed NHPs after intraportal transplantation of xenogeneic porcine islets. Our data suggests that CXCR3-mediated chemotaxis via IP-10 and Mig, expressed at the graft site, is associated with T cell recruitment within 72 h after transplantation. In contrast to CXCR3, CCR5 showed only a marginal increase over time indicative of a relatively less prominent role for CCR5 in porcine xenoislet rejection in NHPs. MIP-1 $\alpha$  and RANTES, which were also previously shown to be important chemoattractants at the islet xenograft site, may act through chemokine receptors other than CCR5. The upregulation of MCP-1 is consistent with findings in murine allo- and xenoislet transplants, which demonstrate the importance of the MCP-1/CCR2 driven cell recruitment [19,22,24,26]. Targeting CXCR3-mediated chemotaxis alone and in combination with MCP-1/CCR2-blockade may provide new mechanistic insights for the design of immunotherapeutic protocols in xenoislet transplantation.

#### Acknowledgments

We thank LaRae Peterson for excellent technical assistance and Per Johansson for input on data analysis and review. This study was supported by funds provided by the University of Minnesota Diabetes Institute for Immunology and Transplantation. M. Hårdstedt was supported by The Iacocca Foundation.

#### References

1. SCHMIDT P, KROOK H, MAEDA A et al. A new murine model of islet xenograft rejection: graft destruction is dependent on a major histocompatibility-specific interaction between T-cells and macrophages. *Diabetes* 2003; 52: 1111.
2. KROOK H, HAGBERG A, SONG Z et al. A distinct Th1 immune response precedes the described Th2 response in islet xenograft rejection. *Diabetes* 2002; 51: 79.
3. BUHLER L, DENG S, O'NEIL J et al. Adult porcine islet transplantation in baboons treated with conventional immunosuppression or a non-myeloablative regimen and CD154 blockade. *Xenotransplantation* 2002; 9: 3.
4. CANTAROVICH D, BLANCHO G, POTIRON N et al. Rapid failure of pig islet transplantation in nonhuman primates. *Xenotransplantation* 2002; 9: 25.
5. KIRCHHOF N, SHIBATA S, WIJKSTROM M et al. Reversal of diabetes in non-immunosuppressed rhesus macaques by intraportal porcine islet xenografts precedes acute cellular rejection. *Xenotransplantation* 2004; 11: 396.

6. INSTON NG, COCKWELL P. The evolving role of chemokines and their receptors in acute allograft rejection. *Nephrol Dial Transplant* 2002; 17: 1374.
7. EL-SAWY T, FAHMY NM, FAIRCHILD RL. Chemokines: directing leukocyte infiltration into allografts. *Curr Opin Immunol* 2002; 14: 562.
8. HANCOCK WW, GAO W, FAIA KL, CSIZMADIA V. Chemokines and their receptors in allograft rejection. *Curr Opin Immunol* 2000; 12: 511.
9. ANONYMOUS. User Bulletin No. 2, Relative quantification of gene expression. ABI 7700 Sequence Detection System 1997, updated 2001. Foster City, CA: Applied Biosystem.
10. RAMAKERS C, RUIJTER JM, DEPREZ RH, MOORMAN AF. Assumption-free analysis of quantitative real-time polymerase chain reaction (PCR) data. *Neurosci Lett* 2003; 339: 62.
11. BAR T, STAHLBERG A, MUSZTA A, KUBISTA M. Kinetic Outlier Detection (KOD) in real-time PCR. *Nucleic Acids Res* 2003; 31: e105.
12. EISEN MB, SPELLMAN PT, BROWN PO, BOTSTEIN D. Cluster analysis and display of genome-wide expression patterns. *Proc Natl Acad Sci U S A* 1998; 95: 14863.
13. MURPHY PM, BAGGIOLINI M, CHARO IF et al. International union of pharmacology. XXII. Nomenclature for chemokine receptors. *Pharmacol Rev* 2000; 52: 145.
14. OLSON TS, LEY K. Chemokines and chemokine receptors in leukocyte trafficking. *Am J Physiol Regul Integr Comp Physiol* 2002; 283: R7.
15. HANCOCK WW, LU B, GAO W et al. Requirement of the chemokine receptor CXCR3 for acute allograft rejection. *J Exp Med* 2000; 192: 1515.
16. AGOSTINI C, CALABRESE F, REA F et al. CXCR3 and its ligand CXCL10 are expressed by inflammatory cells infiltrating lung allografts and mediate chemotaxis of T cells at sites of rejection. *Am J Pathol* 2001; 158: 1703.
17. ZHAO DX, HU Y, MILLER GG et al. Differential expression of the IFN-gamma-inducible CXCR3-binding chemokines, IFN-inducible protein 10, monokine induced by IFN, and IFN-inducible T cell alpha chemoattractant in human cardiac allografts: association with cardiac allograft vasculopathy and acute rejection. *J Immunol* 2002; 169: 1556.
18. ABDI R, MEANS TK, LUSTER AD. Chemokines in islet allograft rejection. *Diabetes Metab Res Rev* 2003; 19: 186.
19. SCHROPPEL B, ZHANG N, CHEN P et al. Differential expression of chemokines and chemokine receptors in murine islet allografts: the role of CCR2 and CCR5 signaling pathways. *J Am Soc Nephrol* 2004; 15: 1853.
20. BAKER MS, CHEN X, ROTRAMEL AR et al. Genetic deletion of chemokine receptor CXCR3 or antibody blockade of its ligand IP-10 modulates posttransplantation graft-site lymphocytic infiltrates and prolongs functional graft survival in pancreatic islet allograft recipients. *Surgery* 2003; 134: 126.
21. PAULE MF, MCCOLL SR, SIMEONOVIC CJ. Murine chemokine gene expression in rejecting pig proislet xenografts. *Transplant Proc* 2000; 32: 1062.
22. SOLOMON MF, KUZIEL WA, MANN DA, SIMEONOVIC CJ. The role of chemokines and their receptors in the rejection of pig islet tissue xenografts. *Xenotransplantation* 2003; 10: 164.
23. GAO W, TOPHAM PS, KING JA et al. Targeting of the chemokine receptor CCR1 suppresses development of acute and chronic cardiac allograft rejection. *J Clin Invest* 2000; 105: 35.

24. ABDI R, MEANS TK, ITO T et al. Differential role of CCR2 in islet and heart allograft rejection: tissue specificity of chemokine/chemokine receptor function in vivo. *J Immunol* 2004; 172: 767.
25. ABDI R, SMITH RN, MAKHLOUF L et al. (CCR5) in islet allograft rejection. *Diabetes* 5 2002; 2489.
26. LEE I, WANG L, WELLS AD et al. Blocking the monocyte chemoattractant protein-1/CCR2 chemokine pathway induces permanent survival of islet allografts through a programmed death-1 ligand-1-dependent mechanism. *J Immunol* 2003; 171: 6929.
27. SALLUSTO F, LANZAVECCHIA A. Understanding dendritic cell and T-lymphocyte traffic through the analysis of chemokine receptor expression. *Immunol Rev* 2000; 177: 134.
28. SALLUSTO F, LENIG D, FORSTER R et al. Two subsets of memory T lymphocytes with distinct homing potentials and effector functions. *Nature* 1999; 401: 708.
29. UNSOELD H, KRAUTWALD S, VOEHRINGER D et al. Cutting edge: CCR7<sup>+</sup> and CCR7<sup>-</sup> memory T cells do not differ in immediate effector cell function. *J Immunol* 2002; 169: 638.
30. YI S, FENG X, HAWTHORNE W et al. CD8<sup>+</sup> T cells are capable of rejecting pancreatic islet xenografts. *Transplantation* 2000; 70: 896.
31. SODERLUND J, WENNBERG L, CASTANOS-VELEZ E et al. Fetal porcine islet-like cell clusters transplanted to cynomolgus monkeys: an immunohistochemical study. *Transplantation* 1999; 67: 784.
32. YI S, FENG X, WANG Y et al. CD4<sup>+</sup> cells play a major role in xenogeneic human anti-pig cytotoxicity through the Fas/Fas ligand lytic pathway. *Transplantation* 1999; 67: 435.